Geophysical Prospecting

EAGE EUROPEAN ASSOCIATION OF GEOSCIENTISTS & ENGINEERS

Geophysical Prospecting, 2017, **65**, 1380–1397 doi: 10.1111/1365-2478.12473

Transient electromagnetic surveys with unimodal transverse magnetic field: ideas and results

Vladimir S. Mogilatov[1,2]*, Arkadiy V. Zlobinskiy[3] and Boris P. Balashov[3]

[1]*Trofimuk Institute of Petroleum-Gas Geology and Geophysics, Russian Academy of Sciences, 630090 Novosibirsk, Russia,* [2]*Novosibirsk State University, 630090 Novosibirsk, Russia, and* [3]*STC ZaVeT-GEO, 630102 Novosibirsk, Russia*

Received January 2016, revision accepted October 2016

ABSTRACT

The theory behind transient electromagnetic surveys can be well described in terms of transverse magnetic and transverse electric modes. Soundings using transverse magnetic and transverse electric modes require different source configurations. In this study, we consider an alternating transverse magnetic field excitation by a circular electric dipole. The circular electric dipole transmitter is a horizontal analogue of the vertical electric dipole. Offshore surveys using circular electric dipole might represent an alternative to the conventional marine controlled-source electromagnetic method at shallow sea and/or for exploring relatively small targets. Field acquisition is carried out by recording either electric or magnetic responses. Electric responses bear information on the 1D structure of a layered earth and successfully resolve high-resistivity targets in marine surveys. Land-based circular electric dipole soundings are affected by induced polarisation. On the contrary, magnetic responses are absent on the surface of a 1D earth, and as a result, they are very sensitive to any and even very small 3D conductivity perturbations. In addition, they are sensitive to induced polarisation or some other polarisation effects in the subsurface. At present, circular electric dipole transmitters and magnetic receivers are successfully used in on-land mineral and petroleum exploration.

Key words: Electrical prospecting, Transient electromagnetic, Transverse magnetic field, Circular electric dipole, Lorentz's force.

INTRODUCTION

Conventional transient electromagnetic (TEM) surveys are carried out using current loops or grounded lines as transmitters. The best way to understand the difference between the two and, possibly, to find alternative source configurations is to represent the electromagnetic (EM) field as a sum of transverse electric (TE) and transverse magnetic (TM) modes. Strictly speaking, the separation of the field into TE and TM modes is only possible in 1D models, from which horizontally layered earth is the most relevant model in geophysics. Although 1D models are oversimplified, considering separated TE and TM fields enabled arrival to very important practical results. For example, Wait (1986) showed that each mode has completely different sensitivity with regard to thin resistive layers. Separating the modes is also efficient in theoretical developments and demonstrates strong relationship with the source's geometry.

The physical and mathematical background of TEM soundings in a layered earth can be represented by a symmetrical model illustrating the dual (TE–TM) nature of the EM field (Fig. 1). The respective derivations are given in Appendix A. An arbitrary current source considered here is represented by the surface distribution of external (eddy) currents $j_{ext}(x,y)$. Ungrounded ($div\mathbf{j}_{ext} = 0$) horizontal current loops of any geometry generate unimodal TE field. Any

*E-mail: mvecs@ya.ru

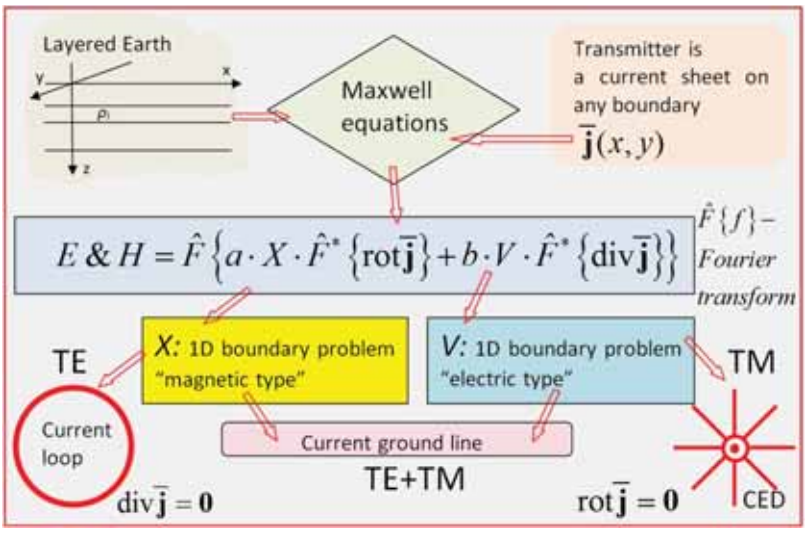

Figure 1 Symmetrical model.

configurations, including grounded current lines ($div\mathbf{j}_{ext} \neq 0$), generate mixed TE–TM fields, except for radial current sources ($rot_z\mathbf{j}_{ext} = 0$), which generate unimodal TM field. Thus, there is an exact antipode producing pure TM field to the conventional horizontal current loops, which produce pure TE field. This is a radial current sheet source called *circular electric dipole* (Mogilatov 1996), configured as a continuum of grounded lines, which is realised in practice as a final set of grounded lines with a common central electrode (Fig. 2). The very important fact is that, in the mixed mode field, the TM mode is much smaller than the TE mode. Therefore, the conventional inductive geoelectrics using horizontal loops and grounded lines is in fact "TE-geoelectrics", whereas the application of unimodal alternating TM fields represents entirely novel "TM-geoelectrics". Although the application of alternating unimodal TEM fields represents a novel approach in geoelectrics, the development of circular electric dipole (CED) transmitters started quite long time ago (Mogilatov 1996; Mogilatov and Balashov 1996). Since then, numerous CED surveys using magnetic field receivers have been conducted in Russia and worldwide and further theoretical development based on multidimensional modelling has been carried out (e.g., Mogilatov *et al.* 2014; Goldman *et al.* 2015; Haroon *et al.* 2016; Mogilatov *et al.* 2016). In addition to the aforementioned CED transmitter, the unimodal TM field can be generated by vertical electric lines (VELs) or vertical electric dipoles (VEDs), which are hard to apply on land and are being developed mainly for marine applications. This alternative to CED will be considered below in greater detail.

ALTERNATING TRANSVERSE MAGNETIC FIELD

Let us consider the difference between the transverse electric (TE) and transverse magnetic (TM) fields by studying

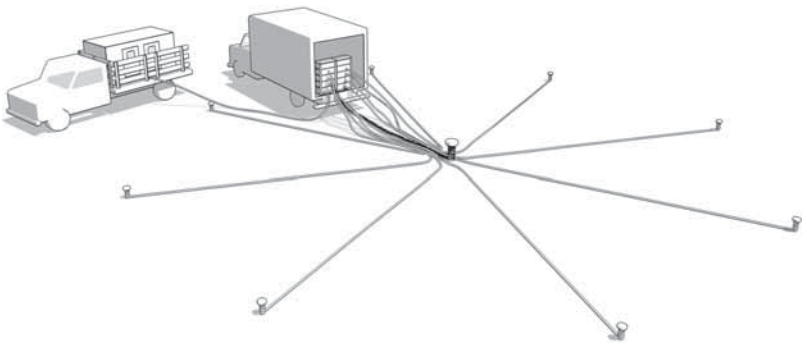

Figure 2 Real Circular Electric Dipole.

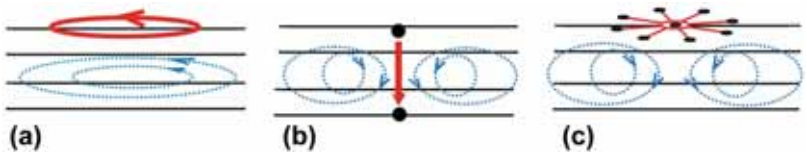

Figure 3 Eddy currents induced by (a) loop, (b) VEL, and (c) CED transmitters (cross-sectional view).

the "pure" responses generated by a horizontal current loop and vertical electric dipole (VED) or circular electric dipole (CED), respectively. The former generates horizontal circular eddy currents and the following three components of the EM field: E_φ, H_r, and H_z (Fig. 3a). On the contrary, VED and CED generate circular magnetic "currents" and, perpendicular to them, a toroidal electric current system with the following field components: H_φ, E_r, and E_z (Fig. 3b and c). In the latter (Fig. 3b and c), only E_r is non-zero on the surface in a quasi-static approximation while the 1D magnetic response is absent (the magnetic field is zero outside the toroidal coil). Thus, the TM and TE modes are principally different both in the way of the interaction between the field and the geological medium and in the configuration (polarisation) of induced eddy currents. This difference is particularly crucial in the time domain.

The late-time ($t \to \infty$) response of a two-layer earth with an insulating basement ($h_1 = h$, $\rho_1 = \rho$, $\rho_2 = \infty$) to loop excitation is (e.g., Wait 1982)

$$E_\varphi(t) \cong M_z \frac{3r}{2\pi S}\left(\frac{\mu_0 S}{2t}\right)^4, \tag{1}$$

where $S = h/\rho$, whereas the loop excitation for VED or CED sources is

$$E_r(t) \cong C \frac{r}{\pi S h^2}\left(\frac{\mu_0 S}{2t}\right)^2 \exp\left(-\frac{\pi^2 t}{\mu_0 S h}\right) \tag{2}$$

$C = I dz_0\, z_0$ and $C = Ib^2/4$ in the case of VED and CED, respectively, where Idz_0 and z_0 are the moment and the position of VED; I and b are the current and the radius of CED (Goldman and Mogilatov 1978; Mogilatov and Balashov 1996). The TE field decays as a power law of time, whereas the TM field decays exponentially. The TE field only depends on the generalised S-parameter, whereas the TM field also depends on depth. Note that the quasi-static approximation is inapplicable to the TM decay in some cases (Mogilatov *et al.* 2014).

Horizontal grounded lines often used in field practice generate both TE and TM fields, but the latter decays quickly, and it is the TE mode that controls the response. In order to extract the important features of the TM field, the residual TE field has to be removed. This procedure can be done analytically (Weidelt 2007), but most efficiently, this is carried out by applying CED or VED.

CIRCULAR ELECTRIC DIPOLE AND VERTICAL ELECTRIC DIPOLE

An alternating transverse magnetic (TM) field generated by surface located circular electric dipoles (CEDs) or immersed within the earth vertical electric dipoles (VEDs) in the presence of the insulating air–earth interface is shown in Fig. 3b and c (secondary currents) and in Fig. 4a (primary currents).

As it was shown earlier, the frequency-domain response of CED on the surface of a 1D earth and that of VED placed at depth z_0 are described by the same vector potential equation if $z_0 \ll r$, $|k_0 r| \ll 1$, and $|\hat{\sigma}_1| \gg \varepsilon_0 \omega$ ($k_j^2 = \mathbf{i}\,\omega \hat{\sigma}_j \mu_0$, $\tilde{\sigma}_j = \sigma_j + \mathbf{i}\,\omega\varepsilon_j$) (see Mogilatov 1996; Appendix B):

$$A_z = \frac{C}{2\pi}\frac{z}{R^3}(1 + k_1 R)\exp(-k_1 R), \tag{3}$$

where $R = \sqrt{r^2 + z^2}$ and C is as in (2). However, as Wait noted in his comment (Wait 1997) to our paper (Mogilatov 1996), both CED and VED should behave as quadrupoles according to equation (3). The CED source is a true quadrupole, whereas VED becomes quadrupole near the ground surface only. If the VED source is immersed within earth or sea, it becomes a dipole (Wait 1982)

$$A_z = \frac{Idz}{4\pi R}\exp(-k_1 R), \tag{4}$$

whereas CED remains quadrupole everywhere (Fig. 4b). The VED source forms a single toroidal system of currents but that of CED has upper and lower components. Therefore, the marine CED and VED transmitters have markedly different patterns of eddy currents as the CED field demonstrates complex behaviour associated with the evolution and interaction of two toroidal systems.

Nevertheless, the CED and VED or vertical electric line (VEL) fields remain similar as long as the two sources are located on and near the ground surface, respectively. So, there is a well-known (see above) relation between the moments of equivalent CED and VEL transmitters:

$$I_{CED}\frac{R^2}{4} = I_{VEL}\, L\, \frac{L}{2} \tag{5}$$

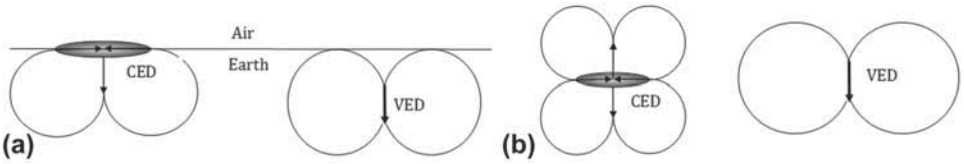

Figure 4 (a) Land-based and (b)marine CED and VED toroidal current systems.

where R is the radius of the CED and L is the length of the VEL. Thus, CED generates exactly the same signals as VEL if $R = \sqrt{2}\ L$. Several publications describing practical applications of marine VEL reported about the sufficient signal-to-noise ratio (SNR) with $L = 1000$ m (Helwig *et al.* 2013; Barsukov and Fainberg 2016; Holten *et al.* 2009). This means that exactly the same SNRs are expected in the considered environments with CED having a radius of approximately 1414 m. It is important to emphasise that, while the VEL moment is limited by the sea depth, the CED might provide a sufficiently high SNR in shallow sea as well.

Calculations using equation (5) for responses to VED and CED excitation show almost coinciding decay curves for an ideal CED and a real one consisting of eight legs radiated from a centre (Fig. 5).

UNIMODAL MARINE TRANSVERSE MAGNETIC FIELD METHODS AS AN ALTERNATIVE AND ADDITION TO CONTROLLED-SOURCE ELECTROMAGNETIC

Methods based on the use of unimodal transverse electric (TE) and/or mixed TE–transverse magnetic (TM) fields are inefficient in the search for deep thin resistive targets such as hydrocarbons and gas hydrates. The only exception represents the marine controlled-source electromagnetic (CSEM) method, which showed excellent signal detectability and vertical resolution with respect to thin resistive targets in deep sea (e.g., Constable and Srnka 2007). However, due to the so-called airwave effect (Weidelt 2007) and huge transmitter–receiver separations, the method is less efficient at shallow sea (although there are some useful features, e.g., Mittet and Morten 2013). Using the above described unimodal TM fields, one can achieve excellent detectability, both vertical and lateral resolutions and all these in shallow and deep oceans. Moreover, it is efficient in case of both resistive and conductive targets. Let us demonstrate this using the "canonical" marine hydrocarbon model (Constable and Srnka 2007) shown in Fig. 6. Let us use CED as a source of a unimodal TM field in the time domain.

Let a CED transmitter be placed either on the seafloor or on the water surface at variable sea depths of 1000 and 100 m. One can see that the target is well detectable in all four cases (Fig. 6). Even in the most unfavourable case, when the CED source is located on the surface of 1000-m-deep water, the maximum relative target response reaches some 1000% (ten times) that is sufficiently high from all points of view.

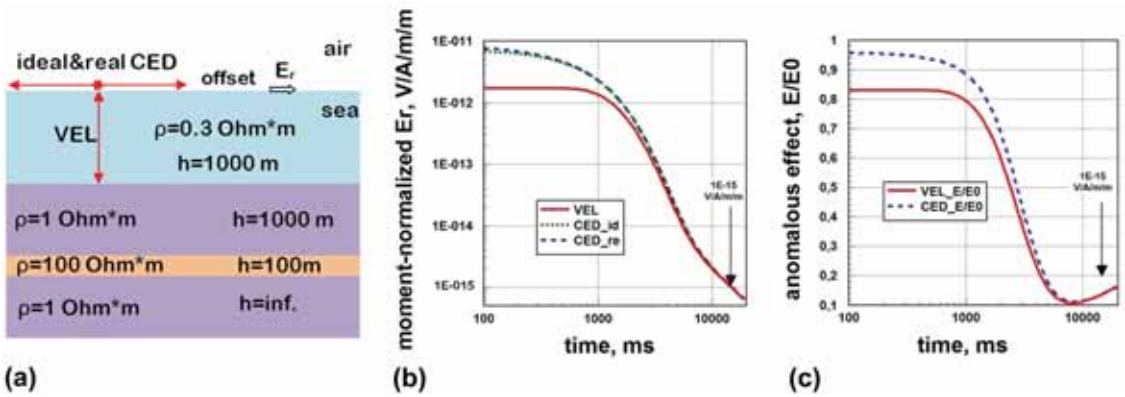

Figure 5 Comparison of the fields of VEL and ideal and real (eight-leg) CEDs. (a) Layered model, (b) voltage decay, and (c) anomalous effects of the thin resistive layer. $L = 1000$ m, $R = 1414$ m, total current $I_{CED} = I_{VEL} = 1000$ A, and offset is 2000 m. Evaluation of the external noise in electric field components is given in (Constable 2010; Flekkøy, Haland and Maløy 2012). The vertical arrow indicates the time at which the responses reach the CED/VEL moment-normalised threshold noise 1E-15 V/A/m/m.

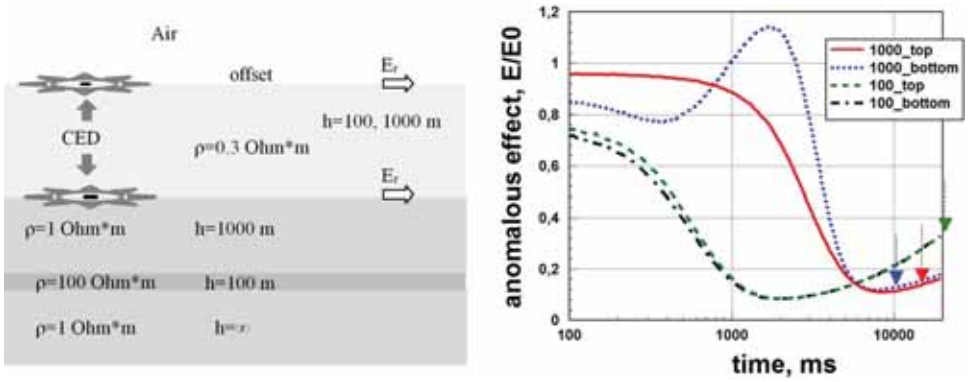

Figure 6 Anomalous effect (E/E_0) in the radial transient electric component, where E is the total CED field and E_0 is the background field (without resistive layer). Radius of CED $R = 1414$ m, total current $I_{CED} = 1000$ A, and offset is 2000 m. 1000_bottom means a CED-E_r on the seafloor at a 1000-m sea depth; 100_bottom means a CED-E_r on the seafloor at a 100-m sea depth; 1000_top means a CED-E_r on the water surface at a 1000-m sea depth; and 100_top means a CED-E_r on the water surface at a 100-m sea depth. The vertical arrow indicates the time at which the responses reach the CED moment-normalised threshold noise 1E-15 V/A/m/m.

We have used the 1D model in the above example. However, if the expected target has limited lateral dimensions, a short-offset configuration might be feasible in the time domain. Comparison of similar models in CSEM (Constable and Weiss 2006; Weiss and Constable 2006) and CED (Goldman *et al.* 2015) shows that CED allows to detect a thin 3D body of a much smaller diameter. In addition, contrary to CSEM, the CED signals are particularly sensitive to the edges of the target. Such option does not exist in standard marine CSEM. Thus, a floating circular electric dipole seems feasible in both deep and shallow seas, as well as for exploring large and small targets.

As for its implementation, it can be done by eight robotic buoy boats unwinding floating wires from winches on the centrally located vessel and GPS-controlled placement of electrodes (Fig. 7). This technology can work on 70% of the Earth's surface.

As far as vertical electric dipole (VED) or vertical electric line (VEL) transmitters are concerned, they were suggested for marine applications a long time ago (Nazarenko 1962). Their feasibility was discussed in a number of earlier (Goldman and Mogilatov 1978) and recent (Um *et al.* 2012; Singer and Artamonova 2013; Goldman *et al.* 2015; Barsukov and Fainberg 2016) publications. Although VED (VEL) is very similar to CED from detectability and resolution points of view, it significantly loses in some other respects. First, the VEL length and, as a result, the signal strength are obviously limited by sea depth. Therefore, similarly to CSEM, it is not that efficient at shallow sea. Another severe limitation of VEL stems from its sensitivity to non-verticality. Measuring the vertical electric gradient (Goldman *et al.* 2015) may help (as the E_z component always belongs to the TM mode) unless there are defects in the vertical measurement line.

The behaviour of signal (voltage in the receive line) as a function of slope (non-verticality) is plotted in Fig. 8 for a 1000-m-long source line and a 50-m-long receive line (offset is 200 m). The source line has a 30 m (~2°) non-verticality of the lower wire end and the receiver line has a ±1.5 m (~2°) non-verticality. Even such minor non-verticality changes the late time response radically. Unlike the TE field, the TM field requires strict source geometry control stricter for 1D (VEL) than for 2D (CED) configurations. Note also that the effect of CED and VEL defects grows non-linearly at smaller sizes.

MAGNETIC FIELD OF CIRCULAR ELECTRIC DIPOLE

Similarly to vertical electric dipole (VED), the background circular electric dipole (CED) magnetic field is zero on the surface of a 1D layered earth and above it. However, the lack of 1D magnetic field in insulating media does not mean that no 1D magnetic field exists in the conductive earth. To prove this statement, let us consider a specific case of a direct current (DC) CED with an infinitely large external radius. Such system is equivalent to a grounded point electrode fed by radial currents. In the coordinates with the origin at the grounded point, its magnetic field in air is well known:

$$H_\varphi^o = \frac{1}{4\pi r}\left(1 - \frac{|z|}{\sqrt{r^2 + z^2}}\right). \quad (6)$$

Since the total magnetic field is zero in the whole upper half-space, the radial currents must produce in the air exactly

Figure 7 Deployment of a floating CED system.

the same field as (6) but with an opposite sign. In the earth, the field of the electrode is the same as in the air, but the field of the radial currents has an opposite sign. Therefore, the total DC magnetic field of CED with infinitely large radius is

$$H_\varphi = \frac{I}{2\pi r}\left(1 - \frac{|z|}{\sqrt{r^2+z^2}}\right). \quad (7)$$

Thus, the quasi-static magnetic field of a CED source is non-zero within the conducting layers of a 1D earth only, and even more so, it does not exist even within conductive structures if they are overlain by any insulating layer. The full cancellation of the background 1D magnetic field on the Earth's surface causes extraordinary sensitivity of the CED method to any lateral resistivity changes within the Earth. This in turn leads to extremely high lateral resolution from one side but to increased sensitivity to geological noise from the other side.

The following numerical example demonstrates the above remarkable feature of the transverse magnetic (TM) field. The left panel in Fig. 9 shows the complicated 3D H-shaped geoelectric target having a resistivity of 1 Ωm located at a depth of 400 m within a conducting half-space having a resistivity of 20 Ωm. The right panel in Fig. 9 shows the calculated transient signal (dB_φ/dt) at the Earth's surface at 9.7 ms. Both the model in the left panel and the calculations in the right panel are produced using program *GeoPrep* (Persova, Soloveichik and Trigubovich 2011). One can see that, even without any processing and interpretation, the contours of the target area delineated fairly well.

Let us compare these results with the appropriate modelling for conventional transverse electric (TE) loop–loop method. Figure 10a shows anomalous dB_z/dt signal, and Fig. 10b shows the total dB_z/dt. One can see that the anomalous TE field provides the detectability and lateral resolution similar to those of CED shown above. However, the actually measured full TE field is entirely different. It provides high detectability due to the very high conductivity of the target but very poor lateral resolution compared with the above TM field. In case of a high-resistivity target, the difference would be even much more pronounced.

However, the use of alternating unimodal TM field allows removing the background effect already in the field, with this being its most valuable advantage.

One can offer CED also in DC (e.g., in MMR) because all the magnetic components (background) are absent on Earth's surface.

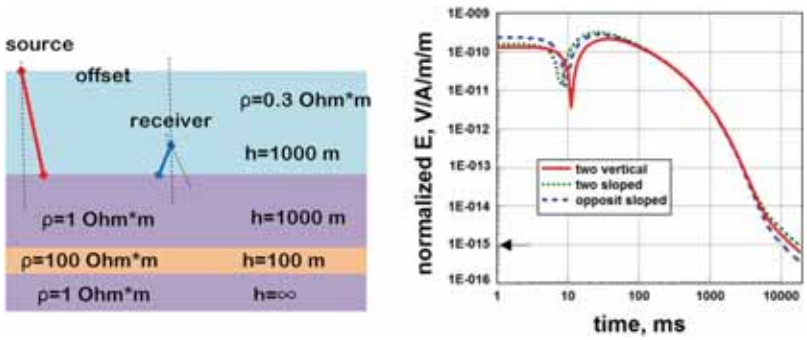

Figure 8 Layered model and the curves of normalised voltage for the VEL–VEL configuration operating with inclined lines. The arrow indicates the normalised threshold noise 1E-15 V/A/m/m.

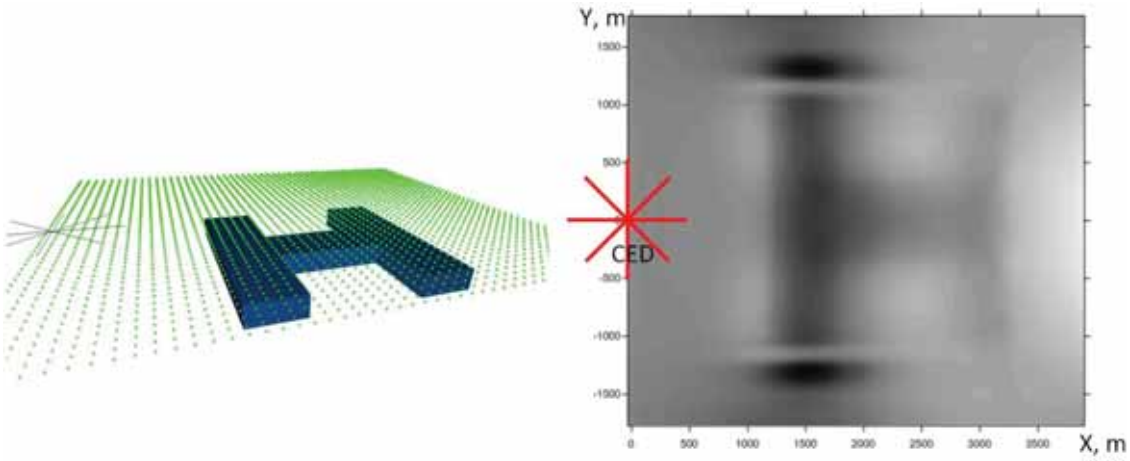

Figure 9 (Left panel) Resistivity model of an H-shaped conductor embedded in a more resistive subsurface. (Right panel) Total field 2D transient response (x,y, t = 9.7 ms). CED-dB_{φ}/dt method.

FIELD SURVEYS WITH A CIRCULAR ELECTRIC DIPOLE SOURCE OF ALTERNATING TRANSVERSE MAGNETIC FIELD

The marine application of circular electric dipole (MCED) is yet a matter of discussions (Goldman *et al.* 2015) while land-based testing of CED systems began in 1993 (Mogilatov and Balashov 1996). Since then, a large amount of data has been acquired with this method, called vertical electric current soundings (VECS), at many ore and oil fields. The key words in the name of the method are "vertical current" because these words emphasise the essential TM feature of the method.

Let us discuss first the problems related to the practical implementation of CED. Contrary to an ideal CED, the real one consists of a final number of radial current lines. Both forward modelling and numerous field experiments show that an ideal CED transmitter is sufficiently approximated by eight current lines. There are two major problems to maintain adequate practical CED: the geometrical symmetry of all current lines and the stable and equal currents in each current line. Through years of research, we have designed the third generation of a transmitter system that maintains equal currents in the eight arms of CED providing a total of 160 A (20 A ± 1% to each arm). The necessary geometrical symmetry is easily maintained using differential GPS in the practical range

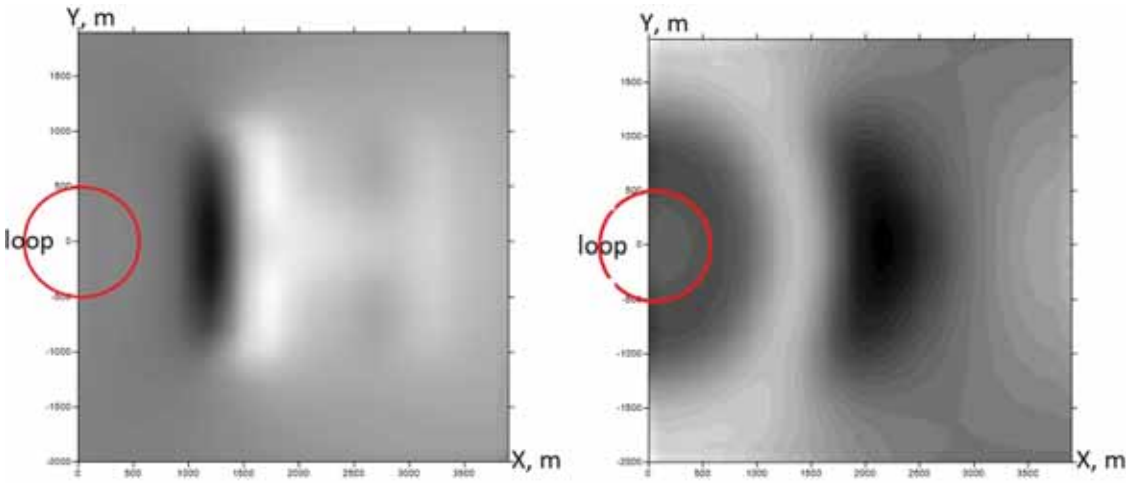

Figure 10 Two-dimensional transient response (x, y, t=9 ms), loop-dBz/dt method: (a) anomaly and (b) total signal.

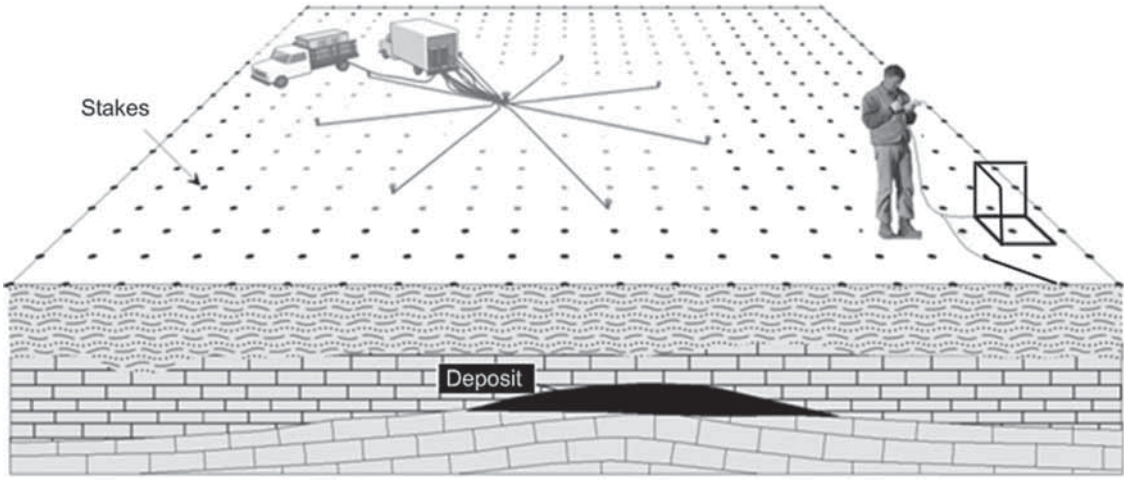

Figure 11 Vertical Electric Current Soundings survey layout: acquiring magnetic and electric transient responses.

of CED radii (between 200 m and 1500 m). For smaller CED, however, providing the necessary symmetry might face a severe technical problem (Haroon *et al.* 2016). Although strictly speaking, the practical CED generates mixed TE–TM field, the TE field is so deeply cancelled in the ground that it causes no effect on real data. As shown above, the voltage decay patterns for an ideal and a real (eight-arm) CED are almost identical (Fig. 5).

As far as the acquisition is concerned, it is possible in two different ways leading to two essentially different methods. The first method is based on measurements of electric field, which bear information on the 1D layered earth structure and, as we have shown above, is highly sensitive to high-resistivity targets in marine surveys. However, in land-based soundings, transient electric responses are strongly affected by induced polarisation (IP), and these measurements were mainly used therefore for studying IP effects.

The second method is based on measurements of magnetic responses, which are absent on the surface of a 1D Earth (see above). As a result, even very weak signals resulted from 3D conductivity perturbations in the subsurface become detectable and might be utilised for contouring mineral or hydrocarbon deposits. Such a technique is most widely used in practice. Fig. 11 shows a typical CED field layout, including a fixed CED transmitter and magnetic sensors measuring dB_z/dt and dB_φ/dt within a large area of up to five CED radii.

It should be noted that numerous important technical issues such as the influence of topography, non-symmetry of CED, and residual TE field are beyond the scope of this paper. These problems have been considered in great detail in Russian language publications (e.g., Mogilatov 2014) and are planned to be considered in our further publications in English. Below, we would like to show two prominent examples of practical application of the VECS method using magnetic sensors (VECS-M) in mineral and hydrocarbon explorations.

VERTICAL ELECTRIC CURRENT SOUNDING METHOD USING MAGNETIC SENSORS IN MINERAL EXPLORATION

The first example shows the results of the vertical electric current sounding method using magnetic sensors (VECS-M) survey using the circular electric dipole (CED)-dB_z/dt and/or CED-dB_φ/dt configurations in the lithium survey near Kaustinen in western Finland (Zlobinskiy and Mogilatov 2014). Lithium (about 1% of LiO_2) occurred in a nearly vertical pegmatite vein, hundreds of metres long and 20–70 m wide, located at a depth from 10 to 200 m. The 15-Ωm pegmatite body was embedded in a 1000-Ωm background (country rocks). In addition, 81 VECS soundings (CED-dB_z/dt) and two background soundings using a horizontal electric line as a transmitter were performed.

The CED transmitter, consisted of eight 200-m-long radial grounded lines, provided a total of 4.5-A current. Transient responses were acquired with an inductive receiver (10000-m^2 effective area) using the *Cycle*-7 measurement system. Theoretical responses of the 3D models were computed using the *GeoPrep* program (Persova *et al.* 2011).

Figure 12 demonstrates all major steps in the interpretation of the data. First, measured signals were visualised as areal maps at different times. The pegmatite vein was marked

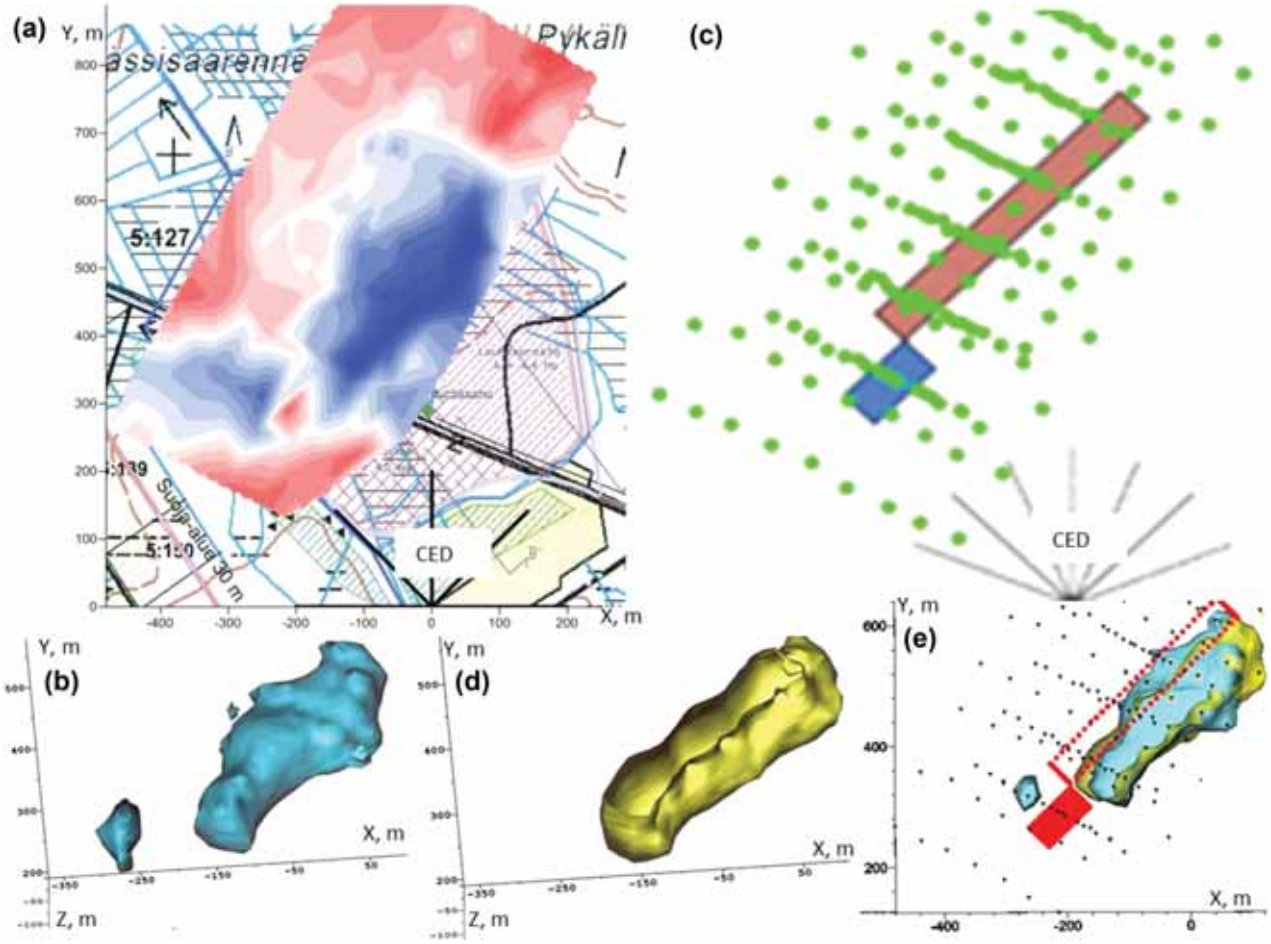

Figure 12 Two- and three-dimensional visualisations of the field and synthetic data cube: (a) 2D field response at 21 μs; (b) 3D visualisation of the field data cube; (c) 3D modelling and choice of model; (d) 3D visualisation of synthetic data; and (e) all targets together.

by sign reversals (Fig. 12a). This step was performed in the field, immediately after completing the data acquisition. The second step included a 3D visualisation ($x,y,t \rightarrow z$) of raw data in the bounds of the marked body. As a result, the 3D image of the object was obtained (Fig. 12b). The follow-up 3D modelling has confirmed the visualisation (Fig. 12d and e).

It should be noted that, due to the high conductivity of the object, it would be successfully delineated by conventional short-offset transient electromagnetic methods (e.g., central loop) as well. However, an acquisition using a fixed transmitter is much less time consuming, and in the case of CED, the resolution of the target is sufficiently high. The survey in question had been carried out in three days, and the target was accurately delineated directly in the field without any complicated processing and interpretation. Moreover, the simple visualisation of the target in the field has significantly facilitated the following rigorous 3D trial and error interpretation of the data. The obtained results proved geophysical and economical efficiency of the VECS-M for delineating highly conductive ore bodies.

VERTICAL ELECTRIC CURRENT SOUNDING METHOD USING MAGNETIC SENSORS IN OIL EXPLORATION

A completely different situation takes place in oil exploration, where the vertical electric current sounding method using magnetic sensors (VECS-M) is expected to be out of competition in detecting and contouring weak lateral conductivity anomalies. In the above considered case of highly conductive ore body, it was easily delineated by VECS-M and the follow-up 3D modelling was entirely consistent with the measured data. In case of oil exploration, however, the results are not supported by conventional modelling, but they are

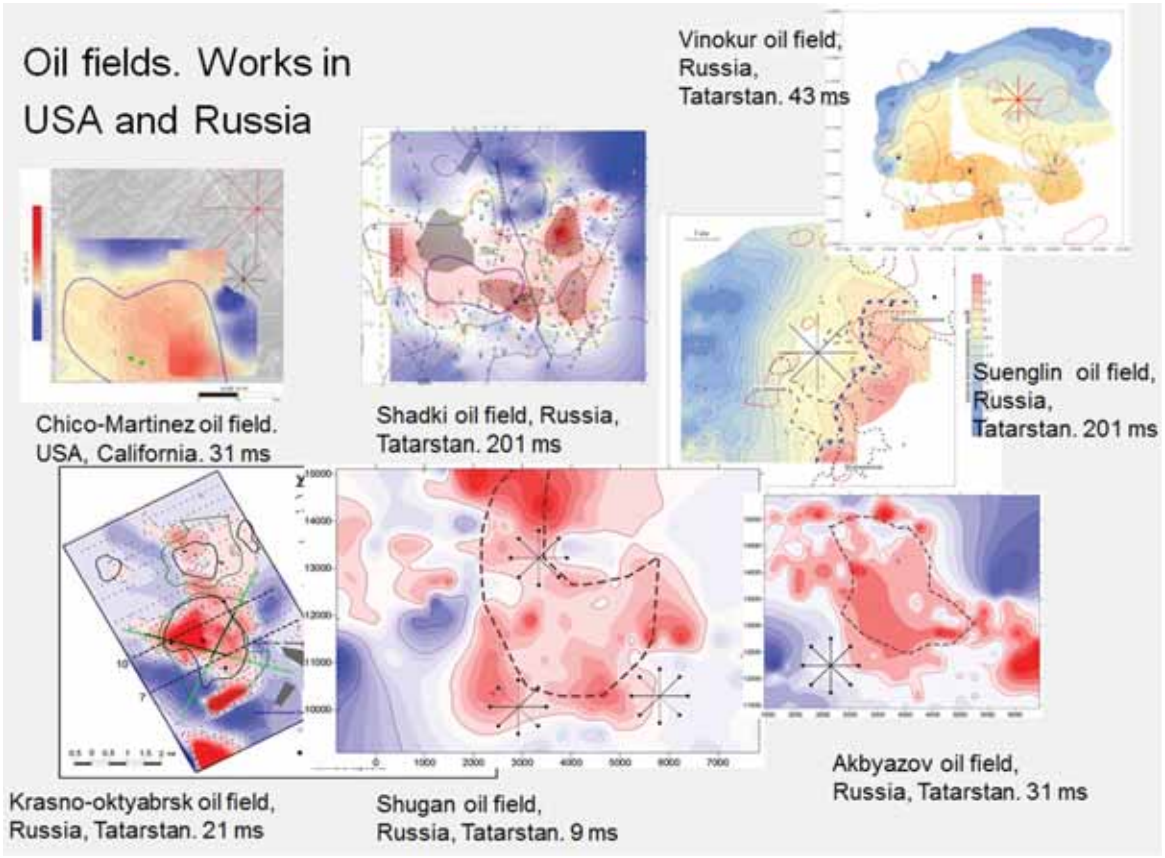

Figure 13 VECS-M in oil exploration (CED-*dBz/dt* transient method). Two-dimensional normalised responses at fixed time above oil fields. (Red) Zone of the positive signal (oil field). (Blue) Zone of the negative signal.

totally consistent with geological and borehole information in all known oil and gas fields used as test sites. All these measurements show increased values of dB_z/dt of the same sign above the oil/gas deposit, whereas the contour of the deposit fits very well with sign reversals of the signal (Balashov *et al.* 2011).

Figure 13 shows the normalised areal VECS-M signals (dB_z/dt) at different measurement times of 9, 21, 43, and 201 ms acquired at well-known oil fields in Tatarstan, Russia. All these fields are characterised by very similar geoelectric conditions. The most prominent feature of the signals is that they are practically independent from measurement times. This means that, in the framework of conventional electromagnetic modelling, the subsurface distribution of properties must have a significant vertical pattern. As an example, Fig. 14b shows a 2D cross section of the data cube (x,y,t or x,y,z) along one of the profiles at the Shadkinskaya oil field. One can see the pillar-alike anomaly just above the known oil deposit (there is also the known 1D background medium, but we do not see it). A similar phenomenon was observed above the Krasno-Oktyabrsk oil deposit (Fig. 13). Due to technical difficulties, a rather low current of 4 A in each leg of circular electric dipole (CED) was injected. As a result, the latest measurement time was just 21 ms, which was far insufficient to achieve the required depth to the target of 1700 m. However, the contours of the deposit were clearly delineated by VECS-M and later on confirmed by follow-up drilling.

Thus, years-long research in attempt to explain the above phenomena with 3D simulations showed the following observations.

- The responses belong to a vertically oriented halo above the oil deposit (Fig. 14) rather than to the deposit itself.
- Even complex conductivity models of oil deposits and their haloes do not explain the stable polarity of responses above the deposit over a large time range.

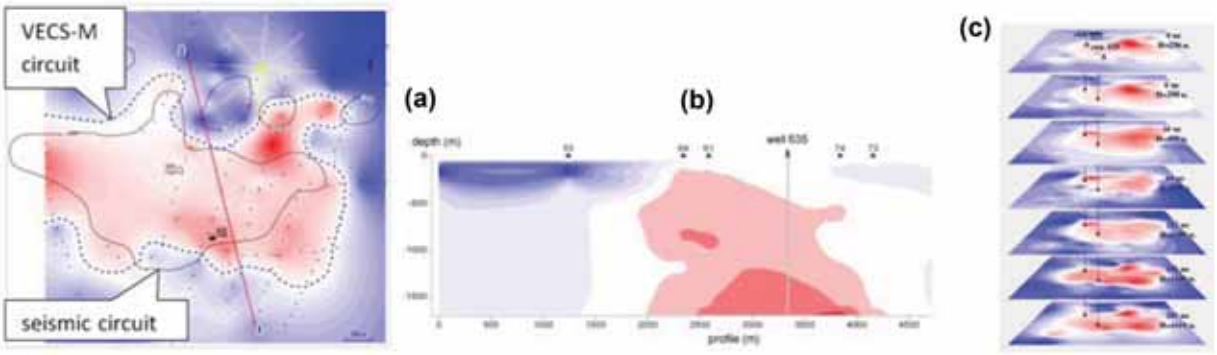

Figure 14 Shadkinskaya field. (a) Two-dimensional normalised response at 201 ms, (b) apparent cross-section of the cube data ($x,y,t \rightarrow z$) along profile I-I, and (c) the series of 2D at different times.

- The Cole–Cole presentation of haloes as anomalous induced polarisation zones likewise leads to responses with sign reversal.

At first glance, it seems that the haloes appear to acquire a magnetic moment during the transient process and become "magnetised" in the nearly vertical direction. However, such explanation is not well substantiated because CED generates only a horizontal magnetic field (H_φ) in Earth. Our preliminary working hypothesis is based on the existence of geomagnetic field, causing increased Lorentz effect in oil haloes (the Hall effect within the Earth, i.e., Hall's anisotropy of the resistivity). It is important to emphasise that haloes (of whichever origin) appear in data of any geoelectromagnetic method, but in conventional methods they remain poorly resolvable against the background. They become well detectable by the suggested VECS-M due to the total absence of the background magnetic field.

APPLICATION OF CIRCULAR ELECTRIC DIPOLE IN ARCTIC

Novel circular electric dipole (CED) transmitters and especially the remarkable features of the generated unimodal transverse magnetic fields open new horizons in geoelectromagnetic

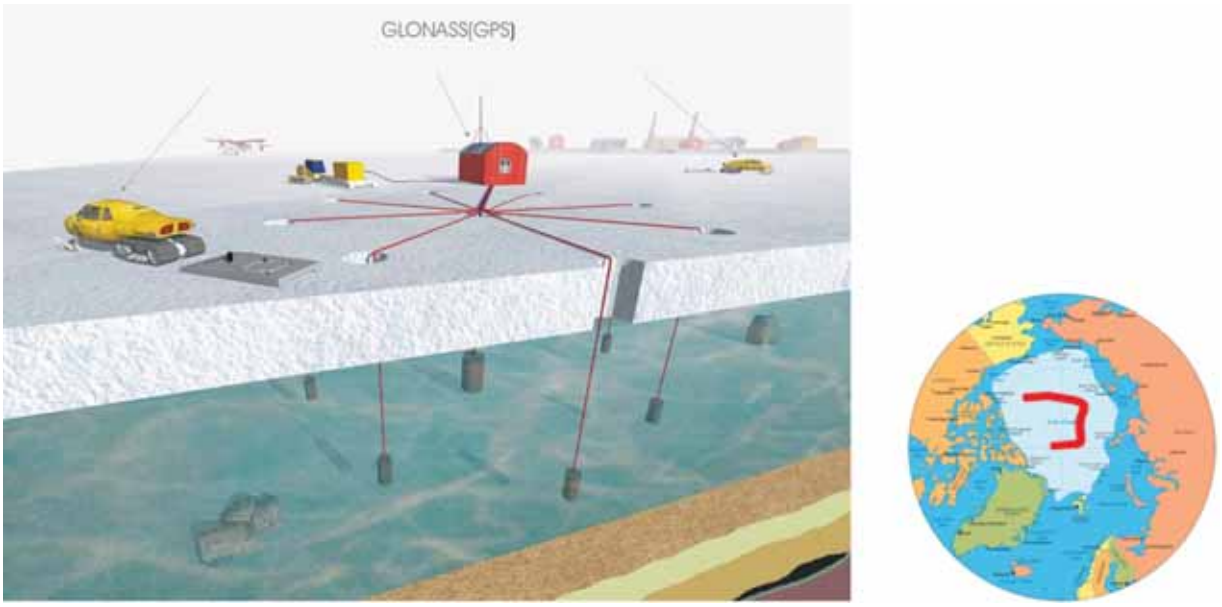

Figure 15 Arctic project: an iceborne Circular Electric Dipole system on drifting ice.

exploration. However, the cumbersome field setup and difficulties in relocation of the transmitter significantly limit both on-shore and marine applications of the method. Fortunately, there is at least one area where the application of CED is not only possible but seems to be incomparably more efficient than any other existing geophysical technique. We are talking about high-latitude Arctic regions permanently covered by drifting ice floes, where the application of any active geophysical method is very difficult to impossible. Paradoxically, such conditions are particularly suitable for applying CED because drifting ice floes, which represent severe obstacles for all other controlled-source electromagnetic methods, are in fact ideal natural platforms for assembling and relocating CEDs. Figure 15 schematically shows the proposed CED system laid out on an ice floe.

The system includes the eight-leg CED transmitter with electrodes grounded in sea water below the ice floe. The signal is picked up by both electrical and magnetic field receivers such as horizontal lines grounded in sea water and horizontal coils (or magnetometers) laid on the ice surface. The measurements are carried out once in a few days or more frequently if the interpretation shows some interesting features. Between the measurements, transmitter batteries are charged using relatively small and lightweight generators. This project is explained in great detail by Mogilatov *et al.* (2016).

CONCLUSIONS

The time-variable unimodal transverse magnetic (TM) field generated by vertical electric dipole (VED) or circular electric dipole (CED) possesses two remarkable features: it is very sensitive to resistive targets, including very thin ones, and its magnetic response measured on the Earth's surface only appears in the presence of 2D/3D structures. Much experience gained in the use of land-based CED shows that it is the only presently available in on-shore source of the unimodal TM field in the frequency and time domains.

The electric field of CED recorded on the surface of a 1D layered earth has exceptional detectability and resolution similar and even exceeding those demonstrated by marine controlled-source electromagnetic. The most important feature of CED, which has been widely tested and applied in the field, is the total absence of the background 1D magnetic response on the surface of the Earth. This exceptional feature of CED allows delineating weak conductivity anomalies (e.g., caused by deep hydrocarbon deposits), which could not be detected by any other existing electromagnetic (EM) method. A few decades ago, geophysicists turned off transmitter current in current conventional transient electromagnetic (TEM) methods to get rid of the annoying direct current background field and achieved high sensitivity and resolution of TEM methods. The proposed CED technology in fact turns off the whole background magnetic response of the subsurface, thus allowing to resolve weak resistivity perturbations, which are practically invisible for conventional EM methods.

ACKNOWLEDGEMENTS

Kind encouragement and support received from the late professor J.R. Wait, as well as his input to CED modelling, are highly appreciated and will be always remembered. The authors would like to thank geophysicists from ZaVeT-GEO company who use the VECS method in their work and the people from Tatarstan who participated in the surveys by VECS for the oil. They would like to specially thank M.G. Persova and Y.G. Soloveichik, experts in 3D simulations.

REFERENCES

Balashov B.P., Mukhamadiev R.S., Mogilatov V.S., Andreev D.S., Zlobinskiy A.V., Shishkin V.K. *et al.* 2011. Vertical electric current soundings for hydrocarbon exploration. *Geofizika* **1**, 61–66.

Barsukov P.O. and Fainberg E.B. 2016. Marine transient electromagnetic sounding of deep buried hydrocarbon reservoirs: principles, methodologies and limitations. *Geophysical Prospecting*.

Constable S. and Weiss C.J. 2006. Mapping thin resistors and hydrocarbons with marine EM methods: insights from 1D modeling. *Geophysics* **71**, G43–G51.

Constable S. and Srnka L.J. 2007. An introduction to marine controlled source electromagnetic methods for hydrocarbon exploration. *Geophysics* **72**, WA3–WA12.

Constable S.C. 2010. Ten years of marine CSEM for hydrocarbon exploration. *Geophysics* **75**(5), 75A67–75A81.

Flekkøy E., Haland E. and Maløy K. 2012. Comparison of the low-frequency variations of the vertical and horizontal components of the electric background field at the sea bottom. *Geophysics* **77**, E391–E396.

Goldman M. and Mogilatov V. 1978. Transient field of a vertical electric dipole embedded in a horizontally layered half-space. In: *Theory and Applications of Electromagnetic Fields in Geophysical Exploration*, pp. 123–138. Novosibirsk: Academy of Science of the USSR.

Goldman M., Mogilatov V., Haroon A., Levi E. and Tezkan B. 2015. Signal detectability of marine electromagnetic methods in the exploration of resistive targets. *Geophysical Prospecting* **63**, 192–210.

Haroon A., Goldman M., Mogilatov V., Bergers R. and Tezkan B. 2016.Exploration of resistive targets within shallow marine environments using the circular electrical dipole and the differential electrical dipole methods: a time-domain modelling study. *Geophysical Journal International* **205**(2), 1032–1048.

Helwig S.L., El Kaffas A.W., Holten T., Frafjord Ø. and Eide K. 2013. Vertical dipole CSEM: technology advances and results from Snøhvit field. *First Break* **31**(4), 63–68.

Holten T., Flekkøy E.G., Måløy K.J. and Singer B. 2009. Vertical source and receiver CSEM method in time-domain. SEG annual meeting, Houston, USA, Expanded Abstracts, 749–752.

Mittet R. and Morten J.P. 2013. The marine controlled-source electromagnetic method in shallow water. *Geophysics* **78**, E67–E77.

Mogilatov V. 1996. Excitation of a half-space by a radial current sheet source. *Pure and Applied Geophysics* **147**, 763–775.

Mogilatov V. 2014. *Pulse Geoelectrics*. Novosibirsk, Russia: Novosibirsk State University, 182 pp.

Mogilatov V. and Balashov B. 1996. A new method of geoelectrical prospecting by vertical electric current soundings. *Journal of Applied Geophysics* **36**, 31–41.

Mogilatov V., Goldman M., Persova M. and Soloveichik Y. 2014. Displacement currents in geoelectromagnetic problems. *Journal of Applied Geophysics* **105**, 133–137.

Mogilatov V., Goldman M., Persova M., Soloveichik Y., Koshkina Y., Trubacheva O. *et al*. 2016. Application of the marine circular electric dipole method in high latitude Arctic regions using drifting ice floes. *Journal of Applied Geophysics*.

Nazarenko O.V. 1962. The apparatus for marine electrical prospecting. *Bulletin of Inventions* **N18**, 1–12.

Persova M.G., Soloveichik Y.G. and Trigubovich G.M. 2011. Computer modeling of geoelectromagnetic fields in three-dimensional media by the finite element method. *Izvestiya, Physics of the Solid Earth* **47**(2), 79–89.

Singer B.S. and Artamonova S. 2013. Vertical electric source in transient marine CSEM: effect of 3D inhomogeneities on the late time response. *Geophysics* **78**, E173–E188.

Um E.S., Alumbaugh D.L., Harris J.M. and Chen J. 2012. Numerical modeling analysis of short-offset electric-field measurements with a vertical electric dipole source in complex offshore environments. *Geophysics* **77**, E329–E341.

Wait J.R. 1982. *Geo-electromagnetism*. New York, NY: Academic Press, 268 pp.

Wait J.R. 1986. Electromagnetic response of a thin layer. *Electronics Letters* **22**(17), 898–899.

Wait J.R. 1997. Letter to editor. Comment on "Excitation of a half-space by a radial current sheet source" by V. Mogilatov. *Pure and Applied Geophysics* **150**, 155.

Weidelt P. 2007. Guided waves in marine CSEM. *Geophysical Journal International* **171**, 153–176.

Weiss C.J. and Constable S. 2006. Mapping thin resistors and hydrocarbons with marine EM methods: Part 2. Modeling and analysis in 3D. *Geophysics* **71**, G321–G332.

Zlobinskiy A.V. and Mogilatov V.S. 2014. VECS soundings for ore exploration. *Geofizika* **1**, 26–35.

APPENDIX A

One-dimensional forward problem of transient electromagnetic soundings

Let an N-layer medium, with the conductivity σ_i , the permittivity, and permeability of the ith layer ($i = 0, 1, \ldots, N$) ε_i and μ_i, respectively (Fig. A-1), be excited by a horizontal current sheet source with the surface density $\mathbf{j}^{\text{ext}}(x, y)\, q(t)$ (in A/m) placed at an interface l ($1 \le l \le N$).

For three sources used in land-based transient electromagnetic (TEM) surveys (horizontal line grounded on both ends or horizontal electric line (HEL) current loop and circular electric dipole or CED), the surface radial eddy current, with non-zero surface density (in A/m), is

$$\begin{aligned}
&\text{HEL}: \; j_x^{\text{ext}}(x, y) = I\, \delta(y)\, [U(x + dx_0/2) - U(x - dx_0/2)],\\
&\text{Loop}: \; j_\varphi^{\text{ext}}(r) = I\, \delta(r - a),\\
&\text{CED}: \; j_r^{\text{ext}}(r) = \tfrac{I}{2\pi r}\, [U(r - r_0 + dr_0/2) - U(r - r_0 - dr_0/2)],
\end{aligned} \tag{A-1}$$

where $U(x)$ is the Heaviside function, $\delta(x)$ is the Dirac delta, dx_0 is the HEL length, a is the loop radius, r_0 is the CED radius, I is the current amplitude, and $r = \sqrt{x^2 + y^2}$.

The Maxwell equations within the layers are continuous on the simple boundaries H_x, H_y, E_x, E_y

$$\begin{aligned}
&\text{rot}\mathbf{H} = \sigma_i \mathbf{E} + \varepsilon_i \frac{\partial \mathbf{E}}{\partial t}, \quad \text{div}\, \mathbf{H} = 0,\\
&\text{rot}\mathbf{E} = -\mu_i \frac{\partial \mathbf{H}}{\partial t}, \quad \text{div}\, \mathbf{E} = 0.
\end{aligned} \tag{A-2}$$

The boundary conditions at $z = z_1$ are

$$\begin{aligned}
&[H_x]\big|_{z=z_l} = -j_y^{\text{ext}}(x, y)\; q(t), \quad [E_x]\big|_{z=z_l} = 0,\\
&\big[H_y\big]\big|_{z=z_l} = j_x^{\text{ext}}(x, y)\; q(t), \quad \big[E_y\big]\big|_{z=z_l} = 0,
\end{aligned} \tag{A-3}$$

where $[F]\,|_{z=z_i}$ means a step on the boundary z_i.

With the horizontal components expressed via the vertical components

$$\begin{aligned}
&\frac{\partial H_y}{\partial x} - \frac{\partial H_x}{\partial y} = \sigma_i E_z + \varepsilon_i \frac{\partial E_z}{\partial t}, \quad \frac{\partial H_x}{\partial x} + \frac{\partial H_y}{\partial y} = -\frac{\partial H_z}{\partial z},\\
&\frac{\partial E_y}{\partial x} - \frac{\partial E_x}{\partial y} = -\mu_i \frac{\partial H_z}{\partial t}, \quad \frac{\partial E_x}{\partial x} + \frac{\partial E_y}{\partial y} = -\frac{\partial E_z}{\partial z},
\end{aligned} \tag{A-4}$$

we obtain two independent problems for the vertical components H_z and E_z as follows: the equations

$$\Delta F = \mu_i \sigma_i \frac{\partial F}{\partial t} + \mu_i \varepsilon_i \frac{\partial^2 F}{\partial t^2}, \qquad F = E_z, H_z, \tag{A-5}$$

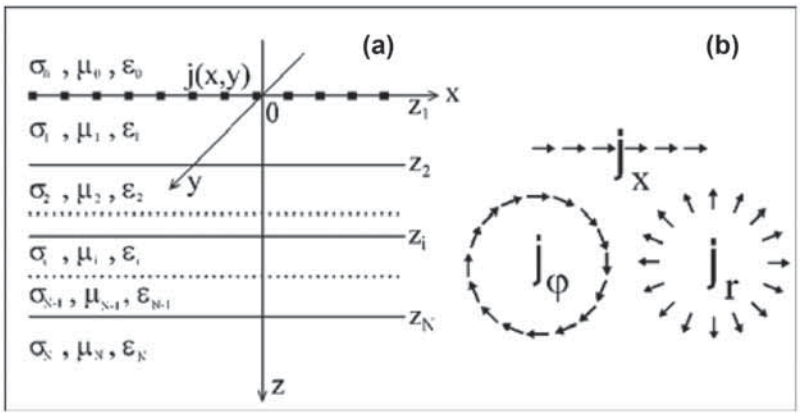

Figure A-1

and the conditions

$$\left[\sigma E_z + \varepsilon \frac{\partial E_z}{\partial t}\right] = \left[\frac{\partial H_y}{\partial x} - \frac{\partial H_x}{\partial y}\right] = \begin{cases} \operatorname{div} \vec{j}^{\,\mathrm{ext}}\, q(t), & i = l \\ 0, & i \neq l \end{cases},$$

$$\left[\frac{\partial E_z}{\partial z}\right]\Big|_{z=z_i} = 0,$$

$$[\mu\ H_z]|_{z=z_i} = 0,$$

$$\left[\frac{\partial H_z}{\partial z}\right] = -\left[\frac{\partial H_x}{\partial x} + \frac{\partial H_y}{\partial y}\right] = \begin{cases} \operatorname{rot}_z \vec{j}^{\,\mathrm{ext}}\, q(t), & i = l \\ 0, & i \neq l \end{cases}. \tag{A-6}$$

Thus, the general problem is separated into two for the transverse electric (TE) and transverse magnetic (TM) modes.

All field components E_x, E_y, E_z, H_x, H_y, and H_z are determined further as Fourier transforms

$$f(x, y, z) = \hat{F}\{f^*(\xi, \eta, z)\} = \frac{1}{4\pi^2}\int\int_{-\infty}^{\infty} f^*(\xi, \eta, z)\mathrm{e}^{\mathrm{i}(\xi x+\eta y)}d\xi\, d\eta, \tag{A-7}$$

and instead of equation (A-4), in each ith homogeneous layer,

$$\begin{aligned} H_x^* &= \bar{\eta}(\sigma_i V + \varepsilon_i \dot{V})D^* + \xi X'_z R^*, \quad E_x^* = \bar{\xi} V'_z D^* - \bar{\eta}\mu_i \dot{X} R^*, \\ H_y^* &= -\bar{\xi}(\sigma_i V + \varepsilon_i \dot{V})D^* + \bar{\eta} X'_z R^*, \quad E_y^* = \bar{\eta} V'_z D^* + \bar{\xi}\mu_i \dot{X} R^*, \\ H_z^* &= XR^*, \quad E_z^* = VD^*, \end{aligned} \tag{A-8}$$

where $\bar{\xi} = \frac{\mathrm{i}\xi}{\lambda^2}$, $\bar{\eta} = \frac{\mathrm{i}\eta}{\lambda^2}$, $\lambda = \sqrt{\xi^2 + \eta^2}$, $(\dot{g})$ and (g'_z) denote time derivatives along z, and the functions

$$R^* = \hat{F}^*\{\operatorname{rot}_z \mathbf{j}^{\mathrm{ext}}\}, \quad D^* = \hat{F}^*\{\operatorname{div} \mathbf{j}^{\mathrm{ext}}\}, \tag{A-9}$$

are the results of inverse Fourier transform of the surface current density:

$$f^*(\xi, \eta, z) = \hat{F}^*\{f(x, y, z)\} = \int_{-\infty}^{\infty}\int f(x, y, z)\mathrm{e}^{-\mathrm{i}(\xi x+\eta y)}dx dy. \tag{A-10}$$

Functions X and V are sought as (series or integral) superpositions of $Z(z)\ \exp(-\alpha t)$ solutions, where $\mathrm{Re}\,\alpha \geq 0$. Parameter α is commonly used as $\mathrm{i}\omega$. Variable ω has a continuous range of values, and functions X and V are represented by Fourier integrals:

$$\left.\begin{matrix} X \\ V \end{matrix}\right\} = \hat{F}(Z) \equiv \frac{1}{2\pi}\int_{-\infty}^{\infty} Q(\omega)Z(z)e^{-\mathrm{i}\omega t}d\omega.\, Q(\omega). \tag{A-11}$$

Function is the transform of the function describing the pulse shape, i.e., $q(t) = \hat{F}(Q)$, and $Q(\omega) = 1/(-\mathbf{i}\ \omega)$ when the current is turned off. At $q(t) = \exp(-\mathbf{i}\omega_0 t)$ (i.e., $Q(\omega) = 2\pi\delta(\omega - \omega_0)$), the solution is sought in the frequency domain. Note that only a discrete spectrum of α and, correspondingly, a Fourier series (Tikhonov's) solution can be obtained under certain conditions (insulating or perfectly conducting half-space top or bottom).

With a source at the boundary $z = z_l$, $(1 \leq l \leq N)$,

$$Z(z) = -\frac{\breve{f}_l}{\breve{f}_l\hat{h}_l - \hat{f}_l\breve{h}_l}\,\breve{\zeta}(z), \quad z \leq z_l \text{ (above source)}, \tag{A-12}$$

$$Z(z) = -\frac{\breve{f}_l}{\breve{f}_l\hat{h}_l - \hat{f}_l\breve{h}_l}\,\hat{\zeta}(z), \quad z \geq z_l \text{ (below source)}. \tag{A-13}$$

Continuous functions f and h are given by

$$\begin{matrix} \text{a) for } X & & \text{b) for } V \\ f = \mu\zeta \quad \text{and} \quad h = \zeta'_z, & & h = (\sigma - \alpha\varepsilon)\zeta \quad \text{and} \quad f = \zeta'_z. \end{matrix} \tag{A-14}$$

Symbols $\breve{f}$ and $\hat{f}$ mean that the function is defined above the source, from the medium top and bottom, respectively, to the boundary with the source.

Thus, expressing $\zeta(z)$ in each layer, successively from top to bottom, via the values at the top, gives

$$\zeta(z) = \zeta_1 \ \exp[u_0(z - z_1)], \quad z \le z_1, \ \text{(in air)},$$
$$\zeta(z) = \zeta_i \ \mathrm{ch}\,[u_i(z - z_i)] + \frac{\zeta'_i}{u_i} \ \mathrm{sh}\,[u_i(z - z_i)], \qquad \text{(A-15)}$$

or expressing $\zeta(z)$ in each layer, successively from bottom to top, via the values at the bottom, gives

$$\zeta(z) = \zeta_{i+1} \ \mathrm{ch}\left[u_i(z - z_{i+1})\right] + \frac{\zeta'_{i+1}}{u_i} \ \mathrm{sh}\left[u_i(z - z_{i+1})\right],$$
$$\zeta(z) = \zeta_N \ \exp[-u_N(z - z_N)], \quad z \ge z_N, \qquad \text{(A-16)}$$

where $u_i^2 = \lambda^2 + k_i^2$, $k_i^2 = -\alpha\mu_i\sigma_i + \alpha^2\mu_i\varepsilon_i$, $(i = 0, 1, \ldots N)$. The value ζ_1 on the boundary above is arbitrary, as well as ζ_N boundary below.

Equations (A-15) and (A-16) represent the known recurrent mechanism for calculating the field in layered media. The algorithm assumes that the source is always located at a boundary (the actual interface in a layered earth or a fictitious one), i.e., there is always at least one boundary.

As an additional remark, a pair of double Fourier transforms (A-7) and (A-10) is equivalent to a pair of Hankel transforms

$$f(r, z) = \frac{1}{2\pi} \int_0^\infty f*(\lambda, z)\, J_0(\lambda, r)\, \lambda d\lambda \qquad \text{and}$$
$$f*(\lambda, z) = 2\pi \int_0^\infty f(r, z)\, J_0(\lambda r)\, r\, dr, \qquad \text{(A-17)}$$

if $f*$ depends on $\lambda = \sqrt{\xi^2 + \eta^2}$, which is valid in our 1D case. The choice between the two transforms is up to the user, depending on configuration and other conditions.

Case 1: current loop

For a circular loop with the radius a, $j_\varphi^{ext}(r) = I\ \delta(r - a)$ in polar and cylindrical coordinates,

$$\mathrm{div}\,\mathbf{j}^{ext} = \frac{1}{r}\frac{\partial j_\varphi^{ext}}{\partial\varphi} = 0,$$
$$\mathrm{rot}_z\mathbf{j}^{ext} = \frac{1}{r}\frac{\partial\left(r j_\varphi^{ext}\right)}{\partial r} = I\ \left[\delta(r - a)/r + \delta'(r - a)\right]. \qquad \text{(A-18)}$$

Consequently, $D^* = 0$ and the source is purely inductive.

Function R^* is determined using the Hankel transform instead of the Fourier transform, taking into account the Dirac delta definition

$$R^* = 2\pi I \int_0^\infty \left[\delta(r - a)/r + \delta'(r - a)\right] J_0(\lambda r)\, r\, dr$$
$$= 2\pi I\ \lambda a J_1(\lambda a). \qquad \text{(A-19)}$$

In cylindrical coordinates, only H_r, H_z, and E_φ are non-zero. For example, E_φ in the ith layer is

$$E_\varphi(r, z, t) = \frac{M_z\mu_i}{\pi\ a} \int_0^\infty J_1(\lambda r)\, J_1(\lambda a)\, \lambda \frac{\partial X(z, t, \lambda)}{\partial t} d\lambda, \qquad \text{(A-20)}$$

where $M_z = I\ \pi\ a^2$ is the source moment. The theory usually considers a loop of an infinitely small radius but with a vertical magnetic dipole at the end. In this case, $J_1(\lambda a) \approx \lambda a/2$ and

$$E_\varphi(r, z, t) = \frac{M_z\mu_i}{2\pi} \int_0^\infty J_1(\lambda r)\ \lambda^2 \frac{\partial X(z, t, \lambda)}{\partial t} d\lambda. \qquad \text{(A-21)}$$

Case 2: circular electric dipole as a galvanic source

A source capable of generating unimodal electric field requires $R^* \equiv 0$ throughout the plane $z = 0$ (in polar coordinates) or

$$\mathrm{rot}_z\vec{j}^{\,\mathrm{ext}} = \frac{1}{r}\left[\frac{\partial(r j_\varphi^{\mathrm{ext}})}{\partial r} - \frac{\partial j_r^{\mathrm{ext}}}{\partial\varphi}\right] = 0. \qquad \text{(A-22)}$$

We obviously arrive at an axisymmetric distribution of eddy current, which has only the radial component $j_r^{\mathrm{ext}}(r)$. Let the eddy-current density be non-zero only near the circle of the radius r_0 (Fig. A-1)

$$j_r^{\mathrm{ext}}(r) = \frac{I dr_0}{2\pi r_0}\ \delta(r - r_0), \qquad \text{(A-23)}$$

where I is the total current. This is the source we call a circular electric dipole (CED). Then,

$$D^*(\lambda) = I dr_0\ \lambda J_1(\lambda r_0), \qquad \text{(A-24)}$$

and the non-zero components of the CED field in the ith layer are

$$H_\varphi(r, z, t) = -\frac{I dr_0}{2\pi} \int_0^\infty J_1(\lambda r) J_1(\lambda r_0)$$
$$\times \left[\sigma_i V(z, t, \lambda) + \varepsilon_i \frac{\partial V(z, t, \lambda)}{\partial t}\right] \lambda d\lambda, \qquad \text{(A-25)}$$

$$E_r(r, z, t) = -\frac{Idr_0}{2\pi}\int_0^\infty J_1(\lambda r)J_1(\lambda r_0)\frac{\partial V(z,t,\lambda)}{\partial z}\lambda d\lambda, \qquad \text{(A-26)}$$

$$E_z(r, z, t) = \frac{Idr_0}{2\pi}\int_0^\infty J_0(\lambda r)J_1(\lambda r_0)V(z,t,\lambda)\lambda^2 d\lambda. \qquad \text{(A-27)}$$

Thus, the CED field is orthogonal to that of the loop. The loop field is TE, and the CED field is TM. The CED field is remarkable by the absence of the quasi-static magnetic response of a horizontally layered earth, as follows from the equations for the H_φ components in the air ($\sigma_0 = 0$). The source we are modelling is a physical idealisation. It is unfeasible in practice to create radial segments of wires of a finite length grounded on concentric circles with radii a and b. In this case, it is necessary to integrate, for example, equation (A-27) along r_0, which leads to

$$E_r(r,\ z,\ t) = \frac{I}{2\pi}\int_0^\infty J_1(\lambda r)[J_0(\lambda b) - J_0(\lambda a)]\frac{\partial V(z,\ t,\ \lambda)}{\partial z}d\lambda.$$

It is convenient to use a central grounded point electrode, i.e., $a = 0$. Moreover, at $b = \infty$, this equation corresponds to an electric field excited by the grounded electrode.

Case 3: grounded line as a mixed source

A grounded horizontal electric dipole (HED) or line is a classical source in TEM surveys. For a short line with the current I grounded at points along the x-axis at $x = -dx_0/2$ and $x = dx_0/2$, the eddy current (on the surface, in A/m), has only the component

$$j_x^{ext}(x, y) = I\ \delta(y)\ [U(x + dx_0/2) - U(x - dx_0/2)],$$

or, for the dipole moment Idx_0,

$$j_x^{ext}(x, y) = Idx_0\ \delta(y)\ \delta(x).$$

Then,

$$\mathrm{div}\ \mathbf{j}^{ext} = Idx_0\ \delta(y)\ \delta'(x), \quad \mathrm{rot}_z\ \mathbf{j}^{ext} = -Idx_0\ \delta'(y)\ \delta(x). \qquad \text{(A-28)}$$

Then, D^* and R^* are

$$D^* = Idx_0\int_{-\infty}^{\infty}\int_{-\infty}^{\infty}\delta(y)\,\delta'(x)\,e^{-i\xi x}e^{-i\eta y}dxdy = Idx_0\ i\xi, \qquad \text{(A-29)}$$

$$R^* = -Idx_0\ i\eta. \qquad \text{(A-30)}$$

Finally, according to equations (A-7)–(A-10) and (A-17), the components of the HED field are

$$\begin{aligned}
H_x &= Idx_0\ \frac{\partial^2}{\partial x\partial y}\hat{Q}\left(\sigma_i V + \varepsilon_i \dot{V} - X'_z\right),\\
E_x &= Idx_0\ \left[\frac{\partial^2}{\partial x^2}\hat{Q}\left(V'_z\right) + \frac{\partial^2}{\partial y^2}\hat{Q}\left(\mu_i \dot{X}\right)\right],\\
H_y &= -Idx_0\ \left[\frac{\partial^2}{\partial x^2}\hat{Q}\left(\sigma_i V + \varepsilon_i \dot{V}\right) + \frac{\partial^2}{\partial y^2}\hat{Q}\left(X'_z\right)\right],\\
E_y &= Idx_0\ \frac{\partial^2}{\partial x\partial y}\hat{Q}\left(V'_z - \mu_i \dot{X}\right),\\
H_z &= Idx_0\ \frac{\partial}{\partial y}\hat{Q}\left(\lambda^2 X\right),\\
E_z &= -Idx_0\ \frac{\partial}{\partial x}\hat{Q}\left(\lambda^2 V\right),
\end{aligned} \qquad \text{(A-31)}$$

where $\hat{Q}$ is the integral operator

$$\hat{Q}(F) = \frac{1}{2\pi}\int_0^\infty J_0(\lambda r)\,\frac{f(\lambda)}{\lambda}d\lambda,$$

and functions X and V satisfy the boundary-value problem (A-7). The representation of the HED field as a sum of the TE and TM components has useful implications for the transient process.

Note that all components except E_z bear a contribution of the TE mode; HED thus becomes an inductive source at late times and thus approaches the loop because the TE mode decays much slower than the TM field.

Our method measuring the purely inductive component H_z actually belongs to TE field surveys. Indeed, it follows from the equations for the horizontal magnetic components H_x and H_y in the air that these components, as well as H_z, are determined only by the magnetic mode in the quasi-static approximation. Thus, any measurements of the magnetic field excited by a current line on and above the surface are methodologically TE field surveys.

APPENDIX B

Field of circular electric dipole in the frequency domain

In fact, this is a brief summary of a personal communication by now deceased James R. Wait first reproduced with his permission in Mogilatov (1996).

In a simple model (Fig. B-1), the radial current sheet (in A/m) is located at the interface between two homogeneous half-spaces. The upper region, z > 0, referred to as the air, has

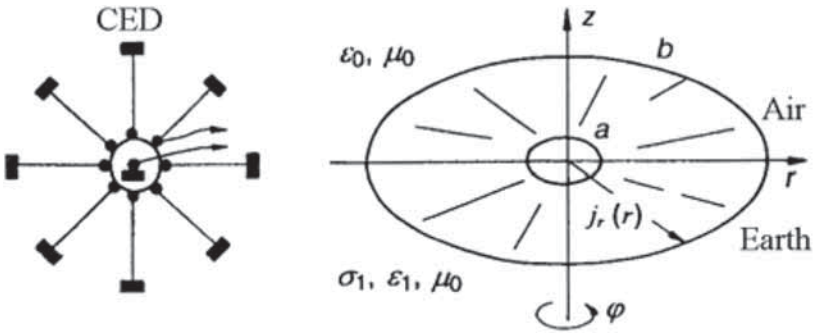

Figure B-1 (Left) Real and (right) ideal CEDs.

the permittivity ε_0 and the permeability μ_0. The lower lossy region, referred to as the earth, has the permittivity ε_1, the conductivity σ_1, and the permeability μ_0. We are to describe the respective fields in terms of the specified source current $j_r(r)$. A time factor $\exp(\mathbf{i}\,\omega t)$ is assumed where ω is the angular frequency.

Because of azimuthal symmetry, the fields can be derived from the vector potential that has only a z component, denoted as A_0 for $z > 0$ and A_1 for $z < 0$. Thus, the non-zero components are

$$E_r = \frac{1}{\tilde{\sigma}_j}\,\frac{\partial^2 A}{\partial r \partial z}, \quad E_z = \frac{1}{\tilde{\sigma}_j}\left(-k_j^2 + \frac{\partial^2}{\partial z^2}\right) A, \quad H_\varphi = -\frac{\partial A}{\partial r}, \tag{B-1}$$

where $k_j^2 = \mathbf{i}\omega\tilde{\sigma}_j\mu_0$, $\tilde{\sigma}_j = \sigma_j + \mathbf{i}\,\omega\varepsilon_j$ $(j = 0, 1)$ and $\sigma_0 = 0$.

The first boundary condition is very simple. It states that E_r is continuous through the plane $z = 0$; thus

$$E_r(z = +0) - E_r(z = -0) = 0. \tag{B-2}$$

The second boundary condition follows from Faraday's law:

$$H_\varphi(z = +0) - H_\varphi(z = -0) = -j_r(r). \tag{B-3}$$

The conditions are met using the integral representations

$$A_0 = \int_0^\infty f_0(\lambda)\exp(-u_0 z) J_0(\lambda r)\,d\lambda, \quad z > 0, \tag{B-4}$$

$$A_1 = \int_0^\infty f_1(\lambda)\exp(+u_1 z) J_0(\lambda r)\,d\lambda, \quad z < 0, \tag{B-5}$$

where $u_j = (\lambda^2 + k_j^2)^{1/2}$ $(j = 0, 1)$. $J_0(\lambda r)$ is the modified Bessel function on the order of 0 and A satisfies the Helmholtz equations $(\nabla^2 - k_j^2)A = 0$.

Now, it remains to determine $f_0(\lambda)$ and $f_1(\lambda)$. Using equations (B-1)–(B-5) gives

$$f_0(\lambda) = \frac{-\tilde{\sigma}_0 u_1 S(\lambda)}{\tilde{\sigma}_1 u_0 + \tilde{\sigma}_0 u_1}, \quad f_1(\lambda) = \frac{\tilde{\sigma}_1 u_0 S(\lambda)}{\tilde{\sigma}_1 u_0 + \tilde{\sigma}_0 u_1}, \tag{B-6}$$

where

$$S(\lambda) = \int_0^\infty j_r(r) r J_1(\lambda r)\,dr. \tag{B-7}$$

Substituting these equations into equations (B-4) and (B-5) gives a formally exact solution valid for any specified radial current density $j_r(r)$. The respective exact expressions for the field components are obtained by derivative operations (B-1).

Let the radial density be

$$\begin{aligned} &j_r(r) = I_0/(2\pi r), \quad a \le r \le b, \\ &j_r(r) = 0, \quad r < a, \quad r > b, \end{aligned} \tag{B-8}$$

where I_0 is the total current flowing across the annular strip. In this case

$$S(\lambda) = \frac{I_0}{2\pi}\int_a^b J_1(\lambda r)\,dr = \frac{I_0}{2\pi\lambda}\,[J_0(\lambda a) - J_0(\lambda b)]\,. \tag{B-9}$$

This form for $S(\lambda)$ would be appropriate for a pair of circular grounded electrodes of radii a and b. To preserve the assumed symmetry, they are being excited by a large number of insulated wires carrying a total current I_0. Of course, at $a \to 0$, we have a point electrode at the centre where. If we further allow $\lambda b \ll 1$ and $J_0(\lambda b) \approx 1 - \lambda^2 b^2/4$, then

$$S(\lambda) \approx \frac{I_0 \lambda b^2}{8\pi}. \tag{B-10}$$

This appears to be a valid approximation for $b \ll r J_0(\lambda a) = 1$ (i.e., the radial coordinate of the observer is much greater than the outer ring electrode), and we assume this to simplify the discussion that follows.

For most geophysical applications, another simplification can be made at $|k_0 r| \ll 1$ (i.e., r is much less than the wavelength in air) and $u_0 \cong \lambda$ so that the fields in the upper air region are valid solutions of Laplace's equation. This is what is meant by the "quasi-static" assumption. However, eddy currents are not ignored. However, the lower earth half-space is assumed to be well conducting in the sense that $|\tilde{\sigma}_1| \equiv |\sigma_1 + \mathrm{i}\,\omega\varepsilon_1| \gg \varepsilon_0\omega$. Under these conditions, equation (A-6) is simplified as follows:

$$f_0(\lambda) \cong -\frac{\tilde{\sigma}_0 u_1 S(\lambda)}{\tilde{\sigma}_1 \lambda}, \quad f_1(\lambda) \cong S(\lambda). \tag{B-11}$$

If we further restrict attention to $a = 0$, and $b \ll$ as aforementioned, expressions (B-4) and (B-5) are further simplified to

$$A_0 \cong -\frac{I_0 b^2}{8\pi}\,\frac{\tilde{\sigma}_0}{\tilde{\sigma}_1}\int_0^\infty u_1 \exp(-\lambda z) J_0(\lambda r) d\lambda,$$

$$A_1 \cong \frac{I_0 b^2}{8\pi}\int_0^\infty \lambda \exp(u_1 z) J_0(\lambda r) d\lambda. \tag{B-12}$$

To deal with the case $z < 0$ (i.e., within earth), we obtain rather simply from equation (B-12) that

$$\begin{aligned} A_1 &= \frac{I_0 b^2}{8\pi}\,\frac{\partial}{\partial z}\int_0^\infty \frac{\lambda}{u_1}\exp(u_1 z) J_0(\lambda r) d\lambda \\ &= \frac{I_0 b^2}{8\pi}\,\frac{\partial}{\partial z}\left[\frac{\exp(-k_1 R)}{R}\right] = -\frac{I_0 b^2}{8\pi}\,\frac{z(1+k_1 R)}{R^3} \\ &\quad \times \exp(-k_1 R), \end{aligned} \tag{B-13}$$

where $R = \sqrt{r^2 + z^2}$.

This final expression for A_1, under the stated assumption, is the same as if the source were replaced by a vertical electric dipole (VED) of current moment Idz located at $z = -h$. With the conditions $h \ll r$, $|k_0 r| \ll 1$, and $|\tilde{\sigma}_1| \gg \varepsilon_0\omega$ (i.e., as for CED), for VED, we have (Wait 1982)

$$A_1 = \frac{Idzh}{2\pi}\,\frac{z(1+k_1 R)}{R^3}\exp(-k_1 R), \tag{B-14}$$

where $z > h$. Equating (B-13) and (B-14) shows that the equivalent electric dipole moment relates to the disc current I_0 by

$$Idzh = I_0 b^2/4. \tag{B-15}$$

This is a remarkable result meaning that the CED is a ground analogue of a vertical electric line at low frequency.